Environment identification and path planning for autonomous NDT inspection of spherical storage tanks

Marco Antonio Simoẽs Teixeira[1], Higor Barbosa Santos[2], Andre Schneider de Oliveira[3], Lucia Valeria Ramos de Arruda[4] and Flavio Neves-Jr[5]

***Abstract*— This paper presents a novel approach to inspection planning in spherical storage tanks by an autonomous climbing robot. The objective is the automatic extraction of some environment characteristics, by robot, to predict the tank dimensions and robot localization. Three distinct perception sources (long range laser rangefinder, light detection and ranging; and depth camera) are used to predict a 3D occupancy grid wrapping calculated tank. From this grid, a path for tank inspection is computed that ensuring a complete icon at the entire tank surface. This scanning must consider kinematic constraints of magnetic wheels and NDT standard. The approach is evaluated in four LPG's spherical tanks virtually designed with same characteristics that real tank projects.**

***Index Terms*— environment identification, path planning, inspection and autonomous climbing robot**

I. Introduction

Mobile robots are a powerful tool to inspect inaccessible and hazardous environments and guarantee repetition and precision that this task requires. Inspection robots should navigate with precision over the whole surface to be inspected to detect any failure or defect.

The spherical tanks used for storage of Liquefied Petroleum Gas (LPG) require frequent inspections and verifications of weld beads and metallic plates during tanks cycle life to prevent failures and leaks. Storage tank inspection usually applies long and expensive techniques, traditionally, through of Non Destructive Technics (NDT). The frequency of inspection is regulated by some international standards and it is the main factor to define insurance and storage costs.

Inspection task traditionally exposes the technicians to unhealthy and often hazardous environments. Mobile robots can be used to reduce or avoid these risks. Inspection robots have the task of navigating through the entire inner and outer surface of storage tank searching for structural failures in the steel plates or weld beads. However, the inspection task cannot be planned if the robot does not know the environment characteristics.

*This project was partially funded by National Counsel of Technological and Scientific Development of Brazil (CNPq), by Coordination for the Improvement of Higher Level People (CAPES) and by National Agency of Petroleum, Natural Gas and Biofuels (ANP) together with the Financier of Studies and Projects (FINEP) and Brazilian Ministry of Science and Technology (MCT) through the ANP Human Resources Program for the Petroleum and Gas Sector - PRH-ANP/MCT PRH10-UTFPR.

[1]all authors are with Federal University of Technology - Parana, Av. Sete de Setembro, 3165, Curitiba, Parana, Brazil

[1]Teixeira, M. A. S. marcoteixeira@alunos.utfpr.edu.br

[2]Santos, H. B. higorsantos@alunos.utfpr.edu.br

[3]de Oliveira, A. S. andreoliveira@utfpr.edu.br

[4]Arruda, L. V. R. de lvrarruda@utfpr.edu.br

[5]Neves-Jr, F. neves@utfpr.edu.br

The environment identification and mapping is currently discussed in the scientific community, mainly to tuning or stabilizing the navigation of mobile robots. [1] discusses a tactile probe designed for surface identification in a context of all-terrain mobile robotic, to adapt the navigation. A similar approach is presented in [2] where a ground classification procedure for a six-legged walking robot is presented. [3] proposes another approach to terrain classification by wheeled mobile robots, which utilizes vibration data. [4] presents the terrain identification based on pressure images generated through direct surface contact by a high-resolution pressure-sensing array.

Legged robots require some informations about terrain to improve the stability of walking motion. The terrain type can be identified by different methods and it allows calculating stiffness, friction and slipping. [5] presents a framework for using a heterogeneous team of legged robots to detect slippery terrain. [6] presents an algorithm to achieve real-time terrain identification and autonomous gait adaptation on a legged robot.

Multi-legged robots, like hexapod topology's, use adaptive behaviors based on surface characteristics to control leg stiffness, slipping and steering control. [7] presents the terrain classification by analysis of characteristic frequency signatures from leg observers, combining current sensing with a dynamic model of the leg motion. [8] discusses an approach for ground classification through estimation errors between commanded and actual positions of each joint. [9] develops a neuromechanical controller through modular neural network and virtual muscle mechanisms.

Industrial manipulators also require knowledge about contact surface to adapt its compliance controller in force tasks. In [10] it is discussed an approach to robotic fingertip to sense object's texture via sliding action.

The odometry of mobile robots can be improved if environment parameters are known, ensuring the pure rolling without skidding and avoiding lateral motion. In [11] it is proposed an approach to improve reliability of odometry of skid-steer mobile robots by robotic terrain classification.

As discussed above, the major part of environment identification approaches currently discussed is focused in improving the navigation or odometry. Path planning also can be enhanced with environment knowledge, because with more information about the surface, more precise will be the planning. In inspection tasks, the path planning is the main requirement, where the robot must cover all surfaces (not only for navigation), but for an accurate inspection.

978-1-5090-3656-1/16 $31.00 © 2016 IEEE
DOI 10.1109/LARS-SBR.2016.39

This work proposes a novel approach to inspection planning of unknown spherical storage tanks, where an autonomous mobile robot extracts several characteristics from environment to predict tank's dimensions and its localization based on three distinct perception sources as a result an occupancy grid is also predicted allow in the inspection planning.The paper is organized as follows. In section 2 the requirements for inspection of storage tanks are discussed. Section 3 presents the Autonomous Inspection Robot and its perception systems. Section 4 describes the whole approach of inspection planning in spherical tanks. In section 5 the benefits of proposed approach are experimentally proved. Section 6 presents the conclusions and future works.

II. Requirements of inspection in storage tanks

Storage tanks, as the ones presented in Fig.1, are metal structures commonly used in industries to store liquids and gases in high pressures. The cylindrical tanks are preferred by some industries due to their reduced installation cost and easier maintenance. However spherical tanks are favored to store great amounts of highly pressurized fluids, such as LPG. The spherical tanks have no corners that would be the weakest region of the structure. These tanks also present lighter and smaller structures compared with cylindrical tanks that have the same load capacity, resulting on layout and operational advantages (smaller area provides less heat exchange with the atmosphere, for example).

Fig. 1: LPG spherical tank.

The inspection of LPG storage tanks is a hazardous and complex task due to the insalubrious environment (especially, inside the tank), size of the inspection area and mainly to the structure height (about 18m). Therefore, an inspection automation process by robot is highly recommended.

During autonomous inspection task, the robot must cover the entire tank's surface and detect the environment's inconsistencies. For this, a climbing robot is designed to navigate in several planes, including the ones perpendicular to the Earth's surface. As a result, the gravitational disturbance is highly important and cannot be neglected during the conception of the robot.

The robot localization on the environment is crucial to inspection because when a surface fault is detected, its exact position must be specified in the tank occupancy grid to maintenance.LPG spheres are fully dark, with no landmarks and no different faces (for any viewpoint the robot will see a semi-sphere), hence, only light-independent perception systems are allowed.

Furthermore, the tank inspection must be planned with precision to ensure that the inspection probe tests the whole surface, without missing areas. However, planning the inspection path without accurate tank informations, such as dimensions and localization, becomes a very complex task.

III. Autonomous Inspection Robot

The robot's mechanical structure is shown in Fig.2. It consists of two parallel sets of fixed wheels (not steerable). Each set is linked by a v-belt, hence two motors control the movement of the four wheels; the robot has two controllable degrees of freedom. Prototype weighs 12kg and the umbilical cord weights 0.4kg/m, it is expected that the robot will carry umbilical cords with length up to 20m.

Fig. 2: Autonomous Inspection Robot (AIR-1).

The robot's wheel sets are misaligned so that, when passing small obstacles (e.g., weld beads), two parallel wheels do not decrease their adhesion forces at the same time. Magnetic wheels were designed so the robot could support its own weight, the inspection equipment and the umbilical cord. Each wheel consists in a set of two ring shaped neodymium magnets positioned between two steel disks and attached by screws with low magnetic permeability. A high hardness polyurethane rubber covers the bonded set. Its magnetic force is approximately 45kgf. More details about the robot's mechanical construction, wheel's concept and magnetic force analysis can be found in [12] and [13].

Robot's perception systems are composed by three main sources. A long-range laser finder (until 70 meters with precision of millimeters) is applied to measure the relative distance between robot and environment, allowing the estimation of tank parameters. A Light Detection And Ranging (LIDAR) is applied to detect any obstacle during navigation. These two perception sources are mounted on a mobile base that can be rotated in roll axis. Finally, a fixed depth camera is used for environment mapping and obstacle detection. The fusion of these sources also promotes a high precision odometry system, as discussed in [14].

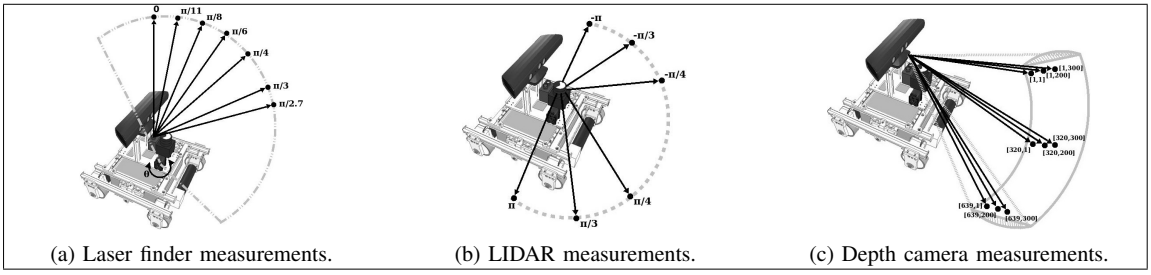

(a) Laser finder measurements. (b) LIDAR measurements. (c) Depth camera measurements.

Fig. 3: Environment perception.

IV. Inspection planning of spherical tanks

The inspection of petroleum derivatives storage tanks only is started after a rigorous planning, that requires some informations about the tank to be inspected. First step of inspection planning is the environment identification, where the Autonomous Inspection Robot (AIR-1) measures the surface and creates a virtual tank model. After that, based on estimated characteristics of the tank, an occupancy grid is predicted to wrapping the tank model, where, each cell stores the reliability of its prediction. Finally, the inspection task is specified in terms of robot's desired path. The proposed approach for inspection planning is designed in some steps, as illustrated in Fig.4. The inspection planning is performed with the robot stopped, i.e., no motion is required. The position and orientation of the robot in relation to the tank is also irrelevant.

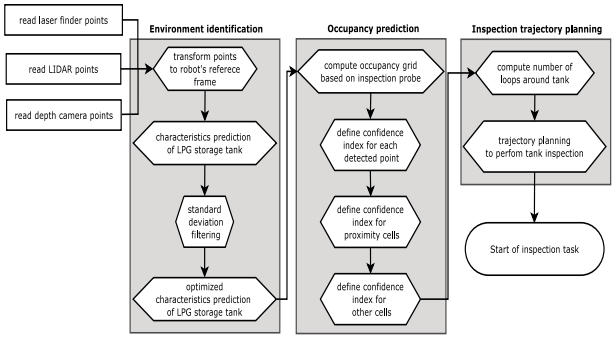

Fig. 4: Inspection planning approach.

A. Environment identification

The environment identification is performed with some measurements through different perception sources, to increase the recognition reliability. Firstly, seven predetermined points are measured with a long-range laser finder (by rotation of mobile base in roll axis), to acquire a set of distant points with high precision, as shown in Fig.3a. Six more points are measured through a LIDAR around yaw axis, illustrated in Fig.3b. Finally, additional nine points are extracted from the depth camera (point cloud) in a mix of roll and yaw axis, as presented in Fig.3c.

Acquired points are measured in relation of coordinate systems fixed on perception sources and they are represented by different viewpoints. It is necessary to transform these points to the same reference system. In this case, the reference system of the robot is fixed on its center. The proposed approach will be independent of the original robot's position and orientation, because it uses the information of inertial measurements to represent transformation between robot center and environment.

The characteristics of the tanks are computed through the use of the least-squares technique, as shown in equation 1. The technique mathematically optimizes a set of data looking for the best fit, minimizing the sum of the squared differences between the estimated and observed data: [15].

$$E = \sum_{i=1}^{m} r_i - r, \tag{1}$$

where, r being the value of the estimated radius and r_i is the observed value.

The radius r can be obtained as

$$r = \sqrt{(x-x_c)^2 + (y-y_c)^2 + (z-z_c)^2}, \tag{2}$$

and observed radius r_i can computed as

$$r_i = \sqrt{(x_i-x_c)^2 + (y_i-y_c)^2 + (z_i-z_c)^2}; \tag{3}$$

where x_c, y_c and z_c represent the center of the sphere; x, y and z represent any point on the sphere; and x_i, y_i and z_i represent a point on sphere with index i.

After definitions of equations 2-3, it becomes possible rewriting equation 1, as

$$E = \sum_{i=1}^{m} \left((x_i-x_c)^2 + (y_i-y_c)^2 + (z_i-z_c)^2 - r^2 \right)^2. \tag{4}$$

The equation 4 can be solved on field of linear algebra, converting the equation to a matrix system and solving the problem $Ax = B$, as

$$A = \begin{bmatrix} 2x_1 & 2y_1 & 2z_1 \\ 2x_2 & 2y_2 & 2z_2 \\ \vdots & \vdots & \vdots \\ 2x_n & 2y_n & 2z_n \end{bmatrix}, \tag{5}$$

$$B = \begin{bmatrix} {x_1}^2 & {y_1}^2 & {z_1}^2 \\ {x_2}^2 & {y_2}^2 & {z_2}^2 \\ \vdots & \vdots & \vdots \\ {x_n}^2 & {y_n}^2 & {z_n}^2 \end{bmatrix}. \tag{6}$$

The sphere center c can be computed as

$$x = \begin{bmatrix} x_c \\ y_c \\ z_c \end{bmatrix} = \Big((A'A)^{-1}A'B\Big) = c \tag{7}$$

The sphere radius sr can be computed as a mean of radius (Eq.2) is defined as

$$sr = \sqrt{\frac{1}{m}\sum_{i=1}^{m}(x_i - x_c)^2 + (y_i - y_c)^2 + (z_i - z_c)^2} \tag{8}$$

B. Occupancy prediction

Occupancy grid is predicted based on an uniform point distribution over computed sphere. For this, the algorithm 1 developed based on works of [16] and [17]. The distribution needs the central sphere point c, the radius r and also the number of points to be distributed m.

Algorithm 1: Tank occupancy prediction.

Input: $c[x,y,z]$ vector of tank center coordinates; r tank radius; n number of points
Output: $o_p[m][3]$ is a $m \times 3$ matrix

Initializations: $o_p[0] \leftarrow [0,0,1]$; $o_p[1] \leftarrow [0,0,-1]$; $i \leftarrow 2$
$d_e = \omega_{sph}\sqrt{\frac{15n+10\pi-\sqrt{225n^2-900n+702.61}-30}{5n+2\pi-10}}$
$n_c \leftarrow \frac{\pi}{d_e} - 1$
$d_d \leftarrow 2\pi\Big(\frac{\sum_{i=1}^{n_c}\sin(d_e i)}{(n-2)}\Big)$
for $i \leftarrow 0$ ***to*** $\big(0.5n_c - 1\big)$ **do**
  $\theta \leftarrow 0 : \frac{2\pi}{\Big(\frac{2\pi}{d_d}\sin\big(\frac{i\pi}{n_c+2}\big)\Big)} : 2\pi$
  $\phi \leftarrow \frac{i\pi}{(n_c+1)}$
  for $j \leftarrow 0$ ***to*** $size(\theta)$ **do**
    $o_p[i,x] \leftarrow \big(\cos(\theta[j])\sin(\phi)\big)r + c[x]$
    $o_p[i,y] \leftarrow \big(\sin(\theta[j])\sin(\phi)\big)r + c[y]$
    $o_p[i,z] \leftarrow \cos(\phi)r + c[z]$
    $\Delta \leftarrow \theta[2] - \theta[1]$
    $o_p[i+1,x] \leftarrow \big(\cos(\theta[j]+\Delta)\sin(\phi)\big)r + c[x]$
    $o_p[i+1,y] \leftarrow \big(\sin(\theta[j]+\Delta)\sin(\phi)\big)r + c[y]$
    $o_p[i+1,z] \leftarrow -\cos(\phi)r + c[z]$
    $i \leftarrow i+2$
return $o_p[m][3]$

where, ω_{sph} is the spherical coefficient $= 1.4142$.

C. Inspection path planning

The inspection path is planned in accord with predicted characteristics of the tank (i.e., center and radius) and it is not influenced by the robot's initial position in relation to the tank. Inspection's motion is designed to minimize angular motion, because the magnetic adhesion system introduces a strong constraint for any lateral motion. The inspection path is composed by several loops around the tank with a small rotation at the beginning, thus, inspecting the whole surface through slices. The distance between each slice is defined by the amplitude of the inspection probe. Full approach for inspection planning is described by algorithm 2.

Algorithm 2: Inspection planning in LPG spherical tanks

Input: $c = [x,y,z]^T$ vector of tank center coordinates; s_r tank radius; s_p size of inspection probe and p_p number of points per loop
Output: $i_{path}[n]$ the vector of 3D points of inspection path

Initializations: $loop \leftarrow \big(\frac{2\pi s_r}{s_p}\big)$; $i \leftarrow 1$
/* computation of tank loops */
for $\varphi \leftarrow 0 : \big(\frac{\pi}{loop}\big)$ ***to*** π **do**
  /* computation of points per loop */
  for $\theta \leftarrow \big(-\frac{\pi}{2}\big) : \big(\frac{2\pi}{p_p}\big)$ ***to*** $\big(\frac{3\pi}{2}\big)$ **do**
    $x \leftarrow \big(c[x] + s_r\cos(\theta)\big)\cos(\varphi)$
    $y \leftarrow \big(c[x] + s_r\cos(\theta)\big)\sin(\varphi)$
    $z \leftarrow \theta$
    /* spartial orientation by unit quaternion */
    $q \leftarrow [\cos(\frac{\varphi}{2}), 0, 0, \sin(\frac{\varphi}{2})]$
    $i_{path}[i] \leftarrow \{x,y,z\}\{q\}$
    $i \leftarrow i+1$
return $ipath$

V. Experimental Results

The proposed approach is evaluated in a set of virtual storage tanks developed with identical characteristics of real tanks, as illustrated by Fig.5. Four LPG spherical tanks with different sizes, layouts and center are used. The real characteristics of virtual tanks as described in table I.

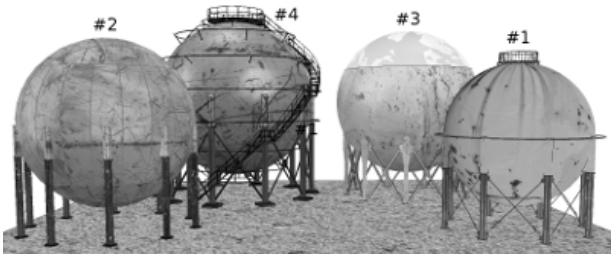

Fig. 5: LPG spherical tank models.

TABLE I: Real characteristics of storage tanks.

Real tank characteristics			
#	volume (m^3)	radius (m)	center (m) [x,y,z]
1	974.02	6.1493	[0,0,6.0649]
2	1596.98	7.2511	[0,0,7.1679]
3	2331.86	8.2263	[0,0,8.1402]
4	3175.37	9.1181	[0,0,9.0329]

Environment identification begins when the inspection robot is put on the tank surface, as seen in Fig.6. The first stage is the surface measuring (i.e., scanning) by perception sources. All measured points are extracted from tank surface and transformed to reference frame fixed on robot's center.

Afterwards, tank dimensions and localization are predicted. Figure 7 presents the influence for each measured

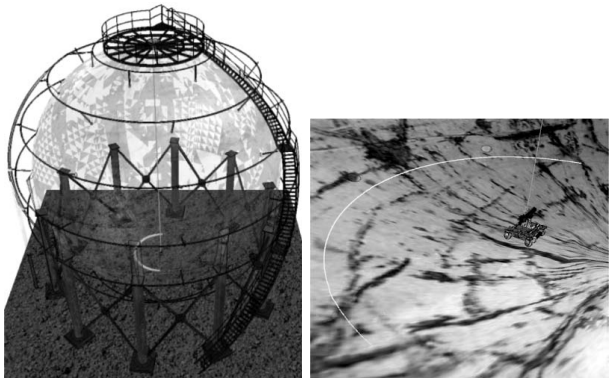

(a) Outside tank. (b) Inside tank.

Fig. 6: Beginning of environment's identification.

point on virtual tanks identification. These identifications start when four points are acquired and it occurs continually until all points are obtained. Points measurement on only one axis (as yaw and roll) does not promote the best tank identification, it is necessary to acquired points from at least two distinct axis. After the acquisition of eight points, the correctness of identification reduces errors around 30 centimeters (Fig.7a). The other points are responsible to reduce error to ten times minor, as seen in Fig.7b.

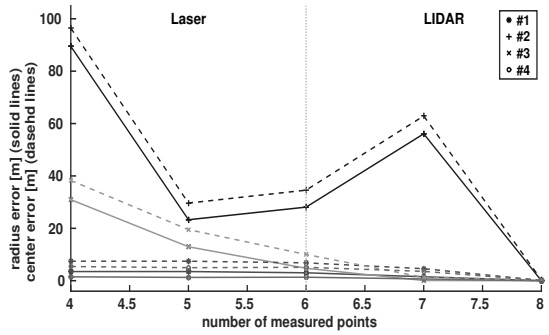

(a) First eight points.

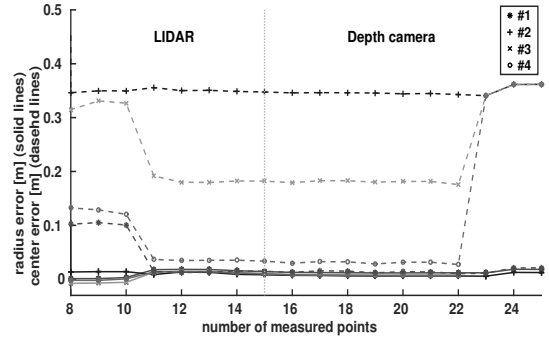

(b) Other points.

Fig. 7: Identification error for each measured point.

The identification method is improved with the filtering of weak points. The deviance filtering is performed applying the standard deviance of all measured points and then discarding all weak points, as presented in Fig.8.

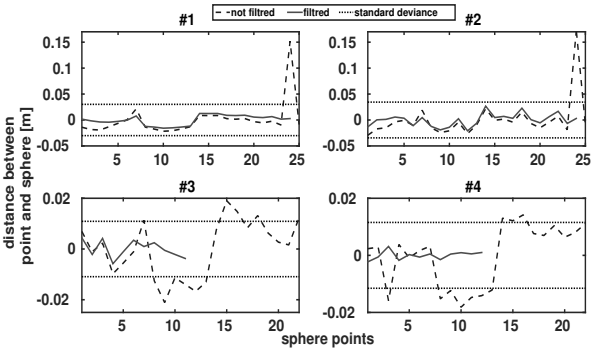

Fig. 8: Weak points filtering based on standard deviance.

The use of most appropriate points promotes a more precise tank prediction, reducing errors when calculating sphere radius and center, as presented in Fig.9.

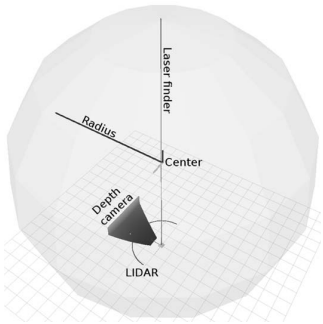

Fig. 9: Tank characteristics extraction.

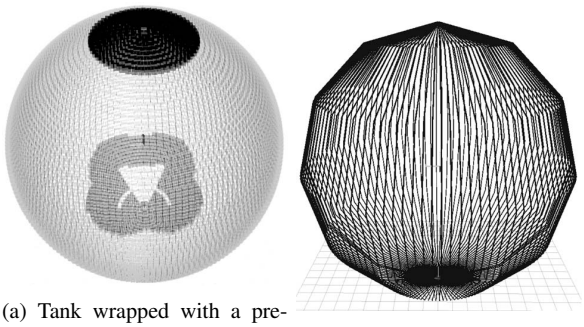

(a) Tank wrapped with a predicted occupancy grid. (b) Inspection path planning.

Fig. 10: Occupancy grid.

The tank is wrapped with a predicted occupancy grid where each cell stores its reliability index. Measured points have higher reliability. Neighboring points of measured points have medium reliability and other points have a lower reliability. Reliability is updated when robot's navigation reach other positions. The initial grid is shown in Fig.10a.

TABLE II: Numerical results of tanks identification.

	not filtred							standard deviation filtering					
#	radius (m)	error (mm)	error (%)	center(m) [x,y,z]'	euclidean distance (mm)	center error (%)	standard deviation (mm)	radius (m)	error (mm)	error (%)	center(m) [x,y,z]'	euclidean distance (mm)	center error (%)
1	6.1675	18.20	0.30	-0.0184 -0.0083 6.0707	20.98	0.35	30.15	6.1613	12.00	0.20	0.0036 -0.0088 6.0631	9.68	0.16
2	7.2635	12.37	0.17	-0.3445 -0.1090 7.1497	361.76	5.05	34.47	7.2569	5.78	0.08	-0.3218 -0.1083 7.1411	340.61	4.75
3	8.2339	7.57	0.09	-0.0488 -0.1688 8.1382	175.94	2.16	10.91	8.2319	5.56	0.07	-0.0451 -0.1642 8.1435	170.32	2.09
4	9.1250	6.91	0.08	-0.0196 -0.0185 9.0281	27.36	0.08	11.53	9.1182	0.17	0.00	-0.0143 -0.0051 9.0311	15.27	0.07

Inspection tasks are specified in a long path around tank surface, designed carefully so the robot covers all of the internal face without any missing area. The planned path is the reference to the navigation controller which ensures a coherent inspection, as illustrated in Fig.10b. All layers inspection plan are presented in robot's viewpoint (Fig.11), including occupancy grid and path planning. A description about numerical tank identification is presented in Table II.

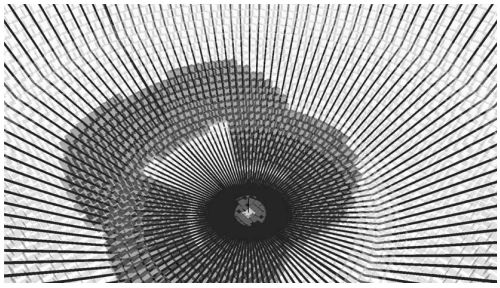

Fig. 11: Planning of robot's viewpoint.

VI. Conclusion

This work discusses an approach to environment identification and inspection planning of an autonomous climbing robot on a LPG spherical storage tank. The inspection task is designed in some steps. Firstly, the tank characteristics are calculated based on a measurement of three distinct perception sources. Afterwards, the occupancy grid is predicted and wrapping in tank to design the 3D mapping in an initial position (without any motion). Finally, the path planning for an inspection task is computed to robot's motion around the tank without missing areas.

Future works will discuss the reliability updating of tank occupancy during robotic navigation and intelligent methods applied to tank identification.

References

[1] P. Giguere and G. Dudek, "A simple tactile probe for surface identification by mobile robots," *Robotics, IEEE Transactions on*, vol. 27, no. 3, pp. 534–544, June 2011.

[2] K. Walas, "Tactile sensing for ground classification," *Journal of Automation Mobile Robotics and Intelligent Systems*, vol. 7, no. 2, pp. 18–23, 2013.

[3] D. Tick, T. Rahman, C. Busso, and N. Gans, "Indoor robotic terrain classification via angular velocity based hierarchical classifier selection," in *Robotics and Automation (ICRA), 2012 IEEE International Conference on*, May 2012, pp. 3594–3600.

[4] J. J. Shill, E. G. Collins, E. Coyle, and J. Clark, "Terrain identification on a one-legged hopping robot using high-resolution pressure images," in *Robotics and Automation (ICRA), 2014 IEEE International Conference on*. IEEE, 2014, pp. 4723–4728.

[5] D. Haldane, P. Fankhauser, R. Siegwart, and R. Fearing, "Detection of slippery terrain with a heterogeneous team of legged robots," in *Robotics and Automation (ICRA), 2014 IEEE International Conference on*, May 2014, pp. 4576–4581.

[6] S. Manjanna and G. Dudek, "Autonomous gait selection for energy efficient walking," in *Robotics and Automation (ICRA), 2015 IEEE International Conference on*, May 2015, pp. 5155–5162.

[7] C. Ordonez, J. Shill, A. Johnson, J. Clark, and E. Collins, "Terrain identification for rhex-type robots," in *SPIE Defense, Security, and Sensing*. International Society for Optics and Photonics, 2013.

[8] G. Best, P. Moghadam, N. Kottege, and L. Kleeman, "Terrain classification using a hexapod robot," in *Proceedings of the Australasian Conference on Robotics and Automation*, 2013.

[9] X. Xiong, F. Wörgötter, and P. Manoonpong, "Neuromechanical control for hexapedal robot walking on challenging surfaces and surface classification," *Robotics and Autonomous Systems*, vol. 62, no. 12, pp. 1777 – 1789, 2014.

[10] V. A. Ho, T. Araki, M. Makikawa, and S. Hirai, "Experimental investigation of surface identification ability of a low-profile fabric tactile sensor," in *Intelligent Robots and Systems (IROS), 2012 IEEE/RSJ International Conference on*, Oct 2012, pp. 4497–4504.

[11] M. Reinstein, V. Kubelka, and K. Zimmermann, "Terrain adaptive odometry for mobile skid-steer robots," in *Robotics and Automation (ICRA), 2013 IEEE International Conference on*, May 2013, pp. 4706–4711.

[12] R. V. Espinoza, A. S. de Oliveira, L. V. R. de Arruda, and F. Neves-Jr, "Navigation's stabilization system of a magnetic adherence-based climbing robot," *Journal of Intelligent & Robotic Systems*, pp. 1–17, 2014.

[13] A. de Oliveira, L. de Arruda, F. Neves-Jr, R. Espinoza, and J. Nadas, "Adhesion force control and active gravitational compensation for autonomous inspection in lpg storage spheres," *Robotics Symposium and Latin American Robotics Symposium (SBR-LARS), 2012 Brazilian*, pp. 232–238, Oct 2012.

[14] R. Veiga, A. S. de Oliveira, L. V. R. Arruda, and F. Neves-Jr, "Localization and navigation of a climbing robot inside a lpg spherical tank based on dual-lidar scanning of weld beads," in *Springer Book on Robot Operating System (ROS): The Complete Reference*. New York: Springer, 2015.

[15] B. Muralikrishnan and J. Raja, *Computational surface and roundness metrology*. Springer Science & Business Media, 2008.

[16] L. Lovisolo and E. Da Silva, "Uniform distribution of points on a hyper-sphere with applications to vector bit-plane encoding," *IEE Proceedings-Vision, Image and Signal Processing*, vol. 148, no. 3, pp. 187–193, 2001.

[17] K. C. Cheung, L. Ling, and S. Ruuth, "A localized meshless method for diffusion on folded surfaces," *Journal of Computational Physics*, 2015.